

# Guiding Errors in 3-Gyro: Experience from WF/PC, WFPC2, STIS, NICMOS and ACS

---

R. L. Gilliland

[gillil@stsci.edu](mailto:gillil@stsci.edu)

February 2005

---

## Abstract

As background information to support interpretation of results during testing under 2-gyro operation, this report summarizes typical behavior gleaned from several observations with ACS, WF/PC, WFPC2, STIS and NICMOS. The observations used have all been for at least five consecutive orbits, and have collected data with the goal of producing very high signal-to-noise, time-series photometry for which definition of x, y offsets in time, and characterization of plate scale changes are an inherent part of the science analysis. In 3-gyro guiding mode it is common to see changes within single orbit visibilities at a level over 10 mas. During the first orbit, and transition to the second, pointing errors are slightly larger than those seen in subsequent orbits. Experience from a total of 385 prime plus parallel orbits is detailed here to give a broad overview of *HST* guiding accuracy.

---

## 1. Introduction

One of the distinct attributes of *HST* capabilities and observations is a remarkable level of pointing and image quality stability in time. Although this report will focus on deviations from perfection, which exist in several forms, *it is worth emphasizing that the*

*overall stability of observations provided by HST is excellent and a prime contributor to successes in many science areas.*

The records described here are intended only to provide a context within which tests in 2-gyro mode can be interpreted compared to nominal experience in 3-gyro. Discussion in this report does not seek to establish causal connections with sources of guiding errors, nor does it seek to establish how accurately information returned in the engineering stream tracks the changes. The purpose of this report is simply to outline with some fidelity the empirical errors in guiding that do occur. Some of the observations described here extended for 100+ contiguous orbits, far longer than any of the 2-gyro tests will last. Results for the full observation sets are provided for completeness, and yield an opportunity to discern possible correlations in guiding, differing between full Guide Star acquisitions versus re-acquisitions, orbits during SAA passages, versus those outside the SAA, and with POS TARGs or without.

## 2. Data Analyzed in this Study

Programs in recent years aimed either at detection of extrasolar planets via transits, or the detailed study of planets transiting bright stars provide ideal support for this study.

The programs used, and time of first observation for each are summarized in Table 1.

General comments on each program are provided here:

GO-4664 A Cycle 3 program spanning 24 contiguous orbits using the PC of WF/PC in September 1993. This was the first substantial use of the CVZ. The core of 47 Tuc was observed in time-series mode using 1000 second integrations with F336W returning high

Table 1: HST Programs with Detailed Guiding Results

Program	Inst.	Orbits	Exps	Exp-time(s)	Start
4664	WF/PC	24	99	1000	1993:247:20:24
8267	WFPC2	123	1289	160	1999:184:15:34
8267	STIS	123	1310	200	1999:184:15:34
9832	NIC3	5	1154	2	2003:317:08:25
9750	ACS/WFC	105	519	339	2004:054:00:05
10441	ACS/HRC	5	108	95	2004:323:13:08

signal-to-noise measurements on 1000s of stars.

GO-8267 A large Cycle 8 program that executed in July, 1999 for 123 consecutive orbits obtaining 160 second exposures on the core of 47 Tucanae in F555W and F814W. Some 34,000 stars were simultaneously observed to S/N of about 100 or higher. The first six orbits were obtained without dithering, while the remainder provided dense coverage of sub-pixel x,y offsets enabling very precise recovery of relative changes in time. Data analysis relied upon producing difference images, which in turn required precise knowledge of x,y offsets and PSF changes in time. The technique is best described in a chapter in Jenkins (2004) which I wrote in support of data analysis plans for the *Kepler* mission, a copy of this chapter can be provided upon request. The relative accuracy of frame-to-frame position offsets is better than a milli-pixel, which is completely irrelevant in comparison to drifts occurring that are over 100 times larger. This generally applies to all of the results described herein: due to the unusually high S/N regime of these observations, measurement errors are negligible. It is possible, though, that systematic errors could exist, for example point spread function changes as a result of OTA breathing could induce correlated pointing offsets, although any such systematic errors are expected to be small compared to the pointing drifts actually experienced.

This program also used STIS in parallel obtaining a comparable number of imaging exposures with the CLEAR and LONGPASS filters. These observations were not formally CVZ, but with visibility windows reaching up to 88 minutes, the observations are near the CVZ. One implication of being in, or near the CVZ is that the scale of differential velocity aberration is at a minimum.

GO-9750 A large Cycle 12 program that executed in February, 2004 for 105 consecutive orbits obtaining 339 second exposures near the galactic bulge in F606W and F814W with the ACS/WFC. Some 50,000 stars were simultaneously observed to a S/N of 100 or better. The analysis approach is similar to that for 8267.

GO-9832 A Cycle 12 program with three sets of five contiguous orbits (only one visit detailed here) each to obtain time-series exposures through transits of HD 209458b with the NICMOS G141 grism. These provide sufficiently high S/N (well over 20,000 summing over the relevant part of the grism bandpass) to attempt detection of water vapor in the planet atmosphere.

GO/DD-10441 A Cycle 13 DD program with three sets of five contiguous orbits (only one set considered here) each obtaining time series photometry of the recently discovered transiting planet system TrES-1. In this case the G800L grism is used with ACS/HRC. Since the spectrum is projected at a steep angle with respect to detector x,y coordinates it

is only possible to accurately measure degenerate shifts in x and y that combine to shift the spectrum, or broaden it in cross dispersion. The results for this program in terms of guiding are discussed in Gilliland (2005). This program is of particular relevance in that it provides data after June 2004 when *HST* started experiencing new behavior – excess jitter during parts of orbits that may be sufficient to alter PSF widths.

### 3. Results and Discussion

The remainder of this ISR will primarily consist of a large number of figures that provide detailed records of relative x,y guiding errors, rotation of detectors relative to target, and plate scale changes. Minimal discussion will be given in the figure captions. The next two subsections provide general conclusions that may be drawn from detailed inspection of the Figures.

#### 3.1. Offsets Within First and Second Orbits

Detailed inspection of offsets *within the first orbit* for programs 4664, 8267, and 9750 show that pointing drift of 10-15 mas within the first visibility window are common. It appears that when first being repointed by a large angle there is a relaxation that leads to significant changes that damp out as a function of time. I have also reviewed offsets within the first orbit for 10 additional visits pulled from followup programs 6473 (December 1997) and 8389 (December 2000) on the original Hubble Deep Field with WFPC2. Unlike the original HDF, these 10 visits were executed as non-contiguous pointings. Of these ten visits, four had offsets between the first two exposures spanning less than one-half of a visibility period of greater than 10 mas up to 14.5 mas – if extrapolated to full visibility periods this suggests drifts for WFPC2 pointings might sometimes reach 30 mas over the initial visibility period.

Similarly the full range of pointing between the start of orbit 1 and the end of orbit 2 is in the range of 15 – 25 mas for 4664, 8267 and 9750, i.e., at a scale comparable to one ACS/HRC pixel or one-half ACS/WFC pixel. On a time scale of 5 – 10 orbits the full range of pointing drift reaches 25-50 mas in these cases with fine temporal sampling.

### 3.2. Accuracy of Dithering

The 8267 and 9750 programs, each of over 100 orbits utilized extensive dithering, but all at small offsets of less than one pixel scale. I will not attempt to quantify the resulting accuracy of these dithers in detail, which numbered approximately 200 over the two programs. Rather, I will simply note that from careful inspection of multi-day pointing error measurements, after subtracting out the applied dithers, the variations remaining show clear changes with a one day period, and stronger variations within orbits, but nothing in evidence that would suggest errors occurring as a result of incorrect offset distances with the POS TARGs commanded. *In this context it is important to recognize that HST does experience significant drifts in terms of objects relative to detector coordinates, this has been true for each of WF/PC, WFPC2, STIS, NICMOS, and ACS. These drifts, on both timescales of a single HST orbit, and separately over many orbits are very large (order of magnitude or more) compared to any errors associated with small POS TARG offsets, and therefore in a practical sense consideration of the possible errors induced during POS TARGs are not relevant.* Stated another way: I believe with large programs it is possible to obtain excellent sub-pixel scale dithering with offsets using random numbers for the dithering, and with a large number of independent offsets. I do not believe that it is possible to specify a desire to obtain offsets that can accurately provide a recti-linear, sub-pixel offset grid to a precision of 10% of a pixel scale, and obtain this in practice – even with use of only small dithers. Furthermore, with the large field and small pixels of ACS/WFC the physical effect of differential velocity aberration would not allow generation of a fine sub-pixel relative offset grid over the full field. This is especially true if trying to realize accurate sub-pixel dithering in the face of drifts within the first few orbits when relaxation to a new pointing provides the largest drift rate.

The original Hubble Deep Field observations provide evidence that the repeatability of dithers over a scale of 1 to 3 arcseconds is excellent. The HDF observations were conducted in the CVZ and involved pointing at the same position for some 10 days. This was the first large program utilizing planned dithering. Within the group setting plans for the dithering there was substantial discussion of how much dithering to do. In the end we compromised at building in just 9 unique dither positions covering a scale of 1 to 3 arcsecs, and with fractional pixel offsets that would *at one position at least in the geometrically distorted WFPC2 field of view* yield a 3×3 sub-pixel grid of dithering as well. Even though most of the 9 dither positions were repeated across time periods of days, *HST* had reached equilibrium at this pointing (flanking field observations were done before the HDF proper), and the pointing was returned to over dithers of 1 – 3 arcsec at the level of 10 mas (see Figure 4 of Williams *et al.* (1996)). The use of only 9 dither positions, coupled with this remarkable repeatability, and the geometric distortion of WFPC2 resulted in some places

in the field of view where most of the sub-pixel dithers fell in a small part of the sub-pixel phase space. Systematics from the resulting poor dithering resulted in the largest errors in forming difference images between the original 1995 HDF observations and my 1997 repeat with just 18 orbits, but with a unique dither each orbit (see discussion in Gilliland, Nugent and Phillips 1999).

## References

- Anderson, J., & King, I. R. 2003, *PASP*, 115, 113.
- Gilliland, R. L., Nugent, Nugent, P. E., & Phillips, M. M. 1999, *ApJ*, 521, 30.
- Gilliland, R. L. 2005, TEL ISR 2005-01.
- Jenkins, J. 2004, Algorithm Theoretical Basis Document for *KEPLER*.
- Williams, R. E. *et al.* 1996, *AJ*, 112, 1335.

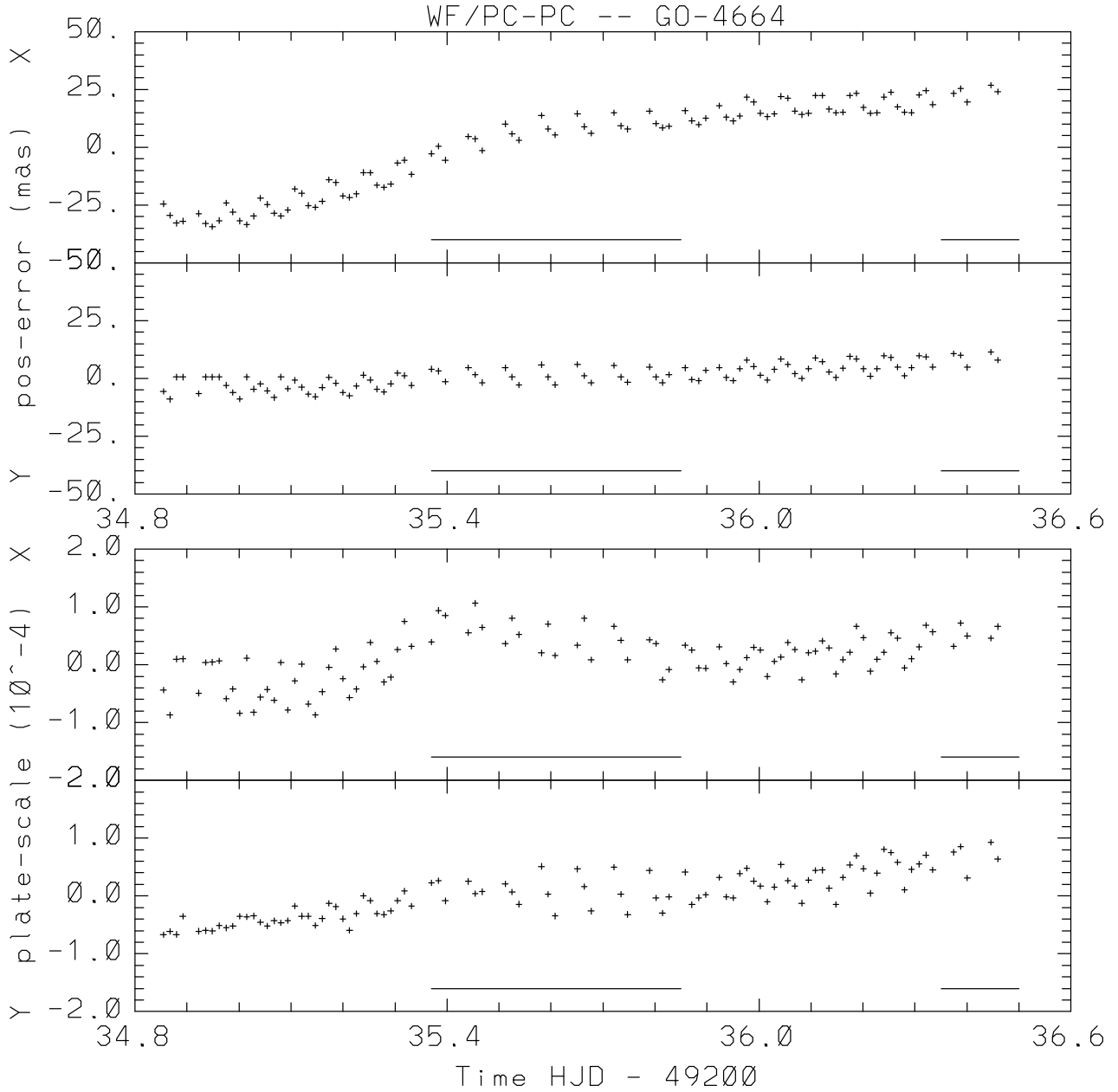


Fig. 1.— Observations with the original WF/PC from September 1993. Individual points represent relative offsets in x and y in the two top panels in units of milli-arcseconds. The lower two panels show plate scale changes at the level of parts in 10,000. Horizontal bars indicate periods of time during which SAA passages occur.

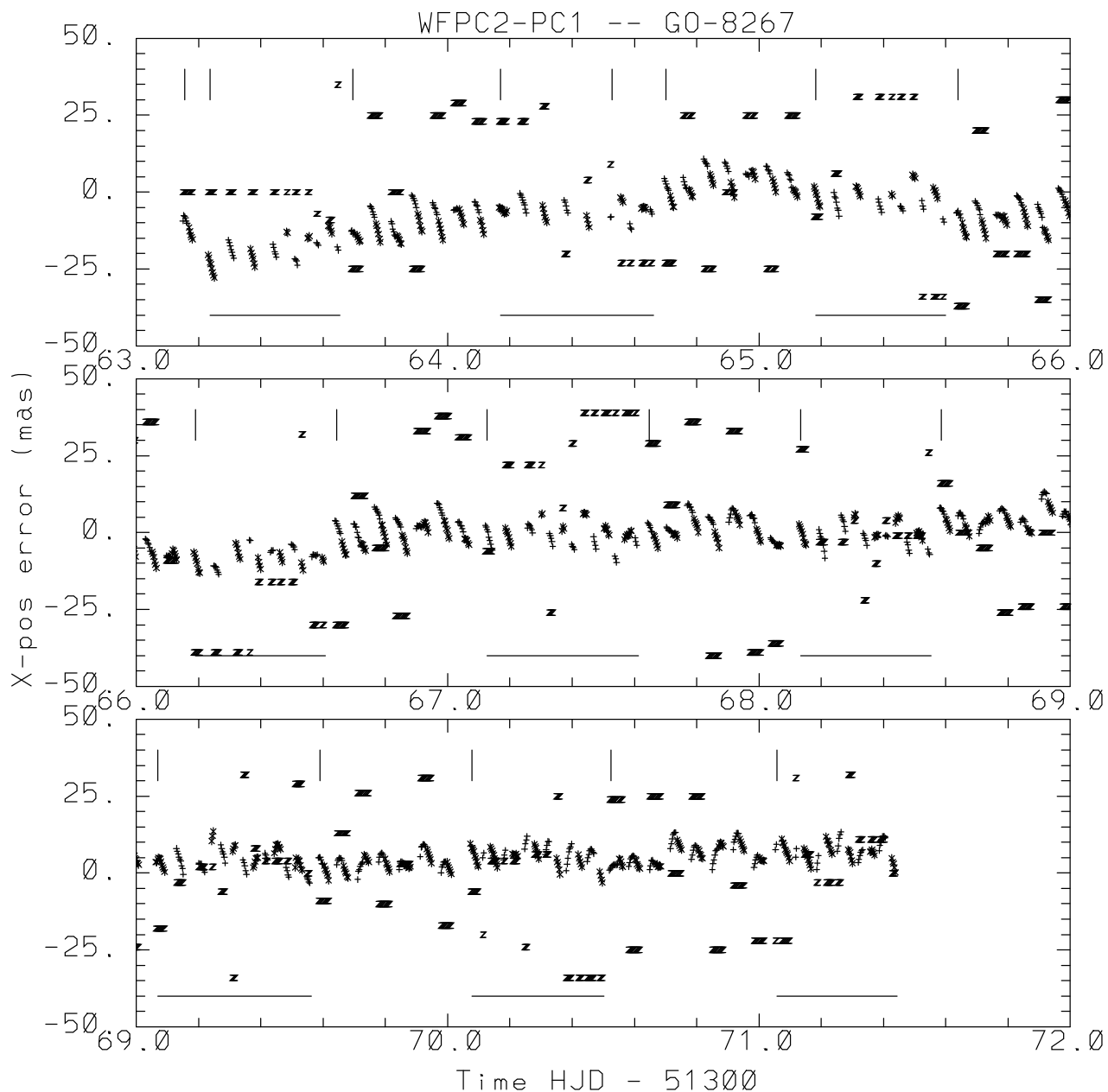


Fig. 2.— The first of five figures covering results from GO-8267 from July 1999. The three panels cover three days each from an 8.3 day period in which only this program executed on the telescope. This page reports X-position offsets in mas after the POS TARG offsets have been removed. The actual POS TARGs are indicated as a series of 'zzzz'. Vertical tic marks indicate times of full GS ACQs, horizontal bars indicate periods of time with SAA passages. F555W observations are shown with '+', while F814W are '\*'. In orbits outside the SAA six exposures in F555W, then six in F814W were obtained in each visibility window.

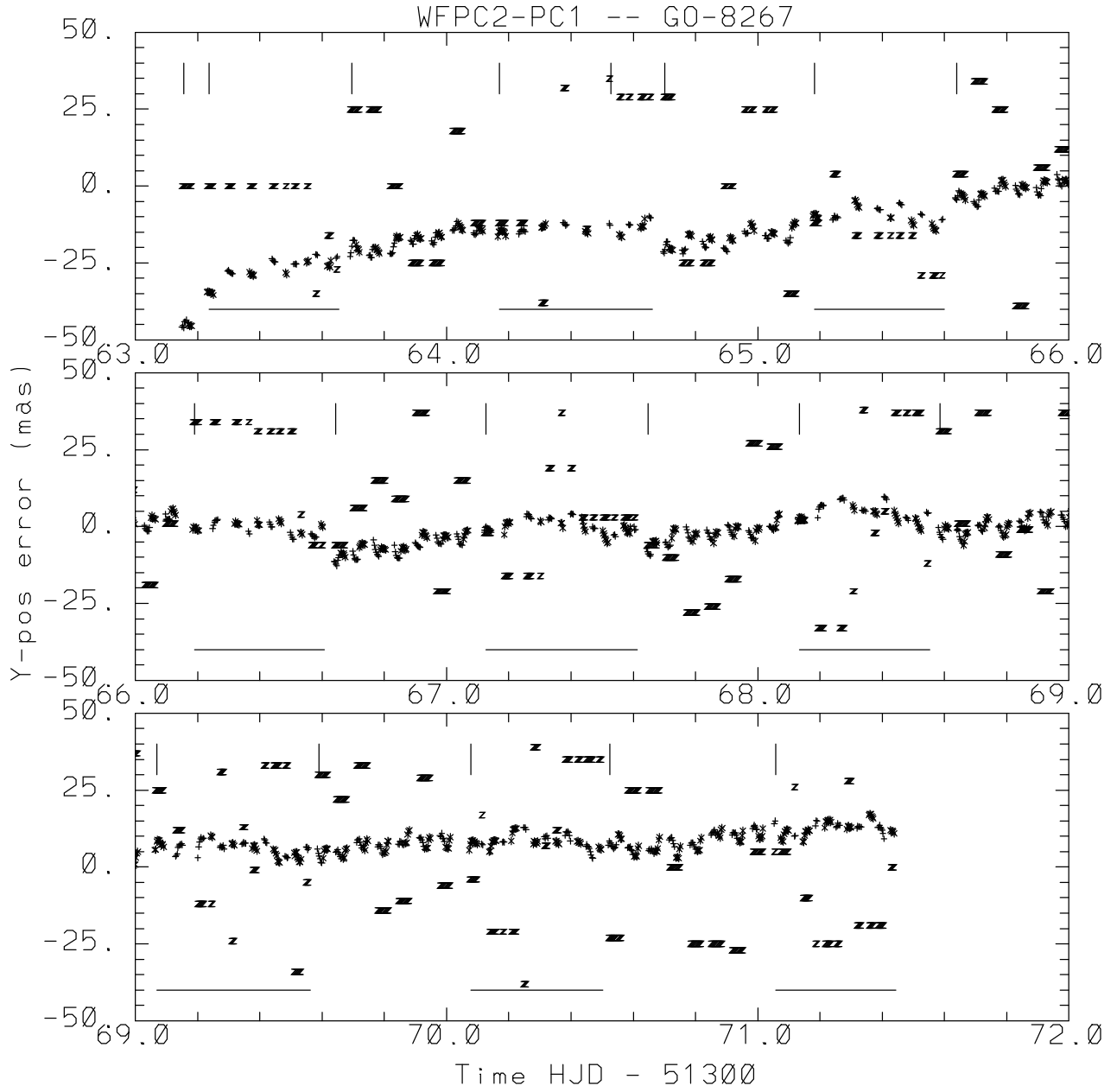


Fig. 3.— Same as Figure 2, but shows offsets in time for the detector y-position.

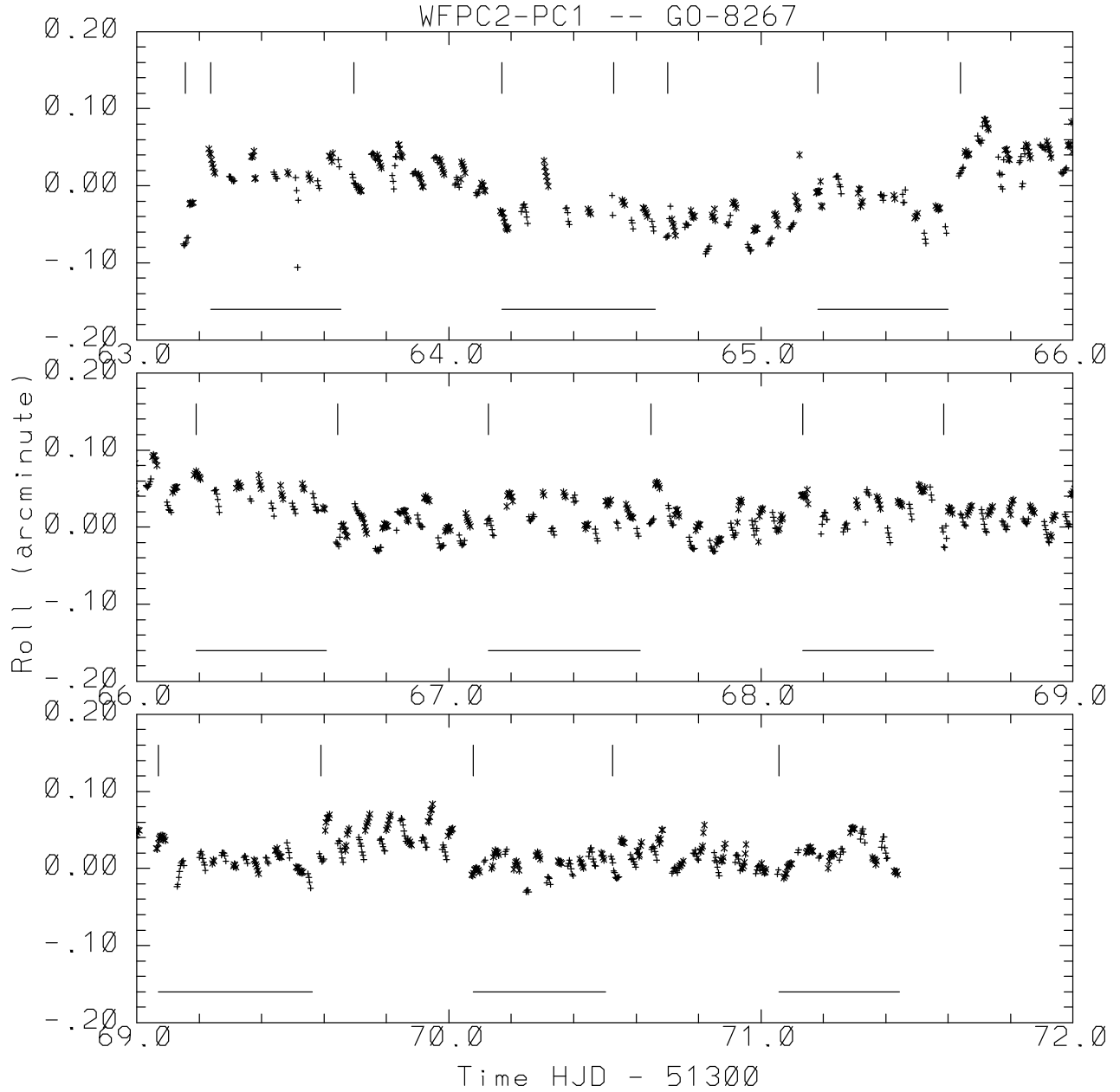


Fig. 4.— Same as Figure 2, but shows rolls of the detector relative to target with an arbitrary zero point. A roll of 0.1 arcminutes corresponds to center to corner offsets of 0.016 pixels for this  $800 \times 800$  pixel detector. These observations used standard pointing control with two guide stars resulting in excellent roll control.

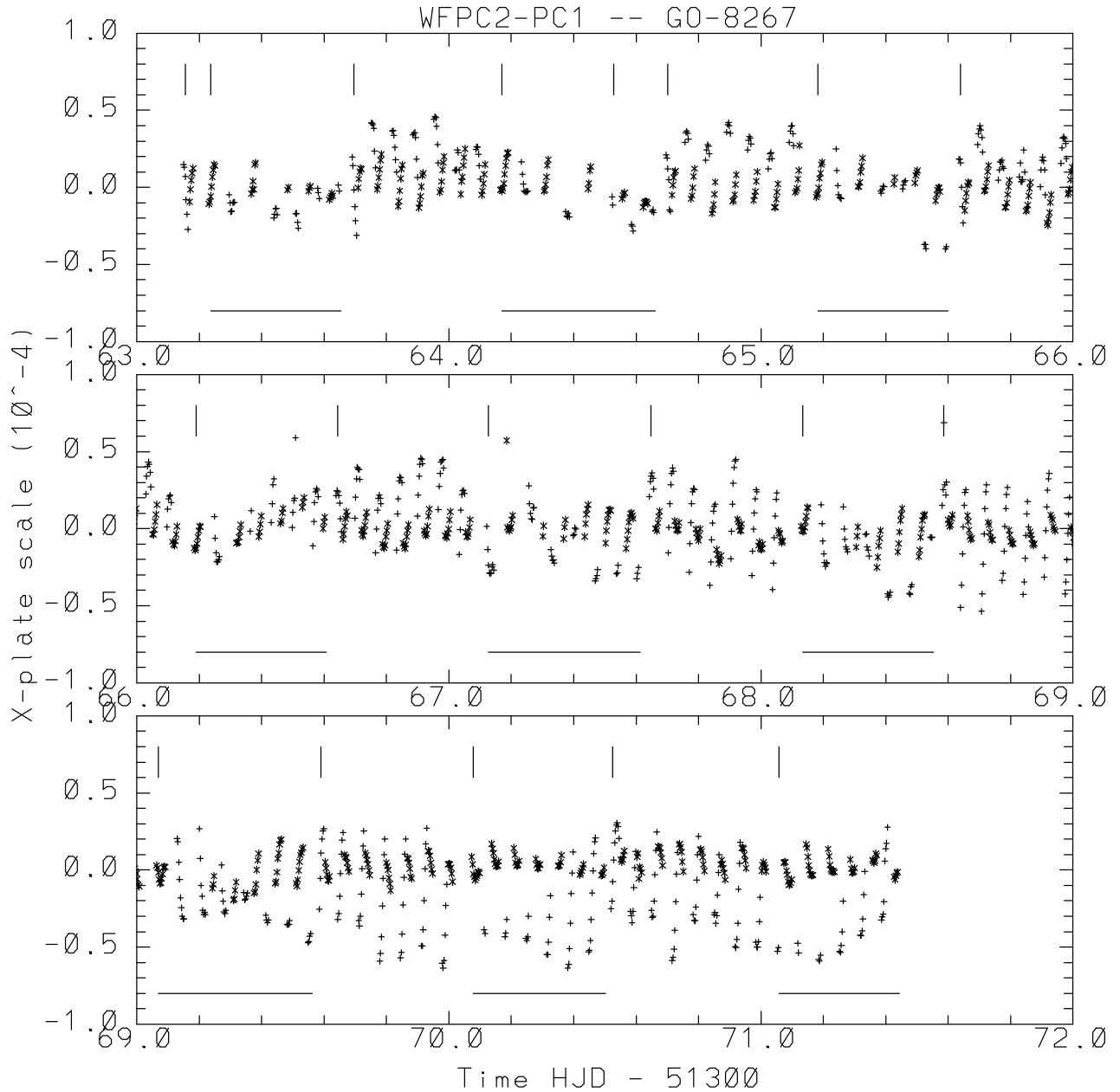


Fig. 5.— Same as Figure 2, but shows the variation of plate scale in the detector x-direction. A plate scale change of  $0.5 \times 10^{-4}$  corresponds to a center-to-edge stretch of 0.02 pixels. Note that differential velocity aberration for the *HST* orbital velocity of 7.5 km/s is at most  $v/c$ , or  $0.25 \times 10^{-4}$ , and for these observations near the pole of the orbit this is further reduced by  $\cos(\text{angle of motion to source})$  which is small for near-CVZ. Most of the plate scale change is not due to velocity aberration (see also Anderson and King 2003).

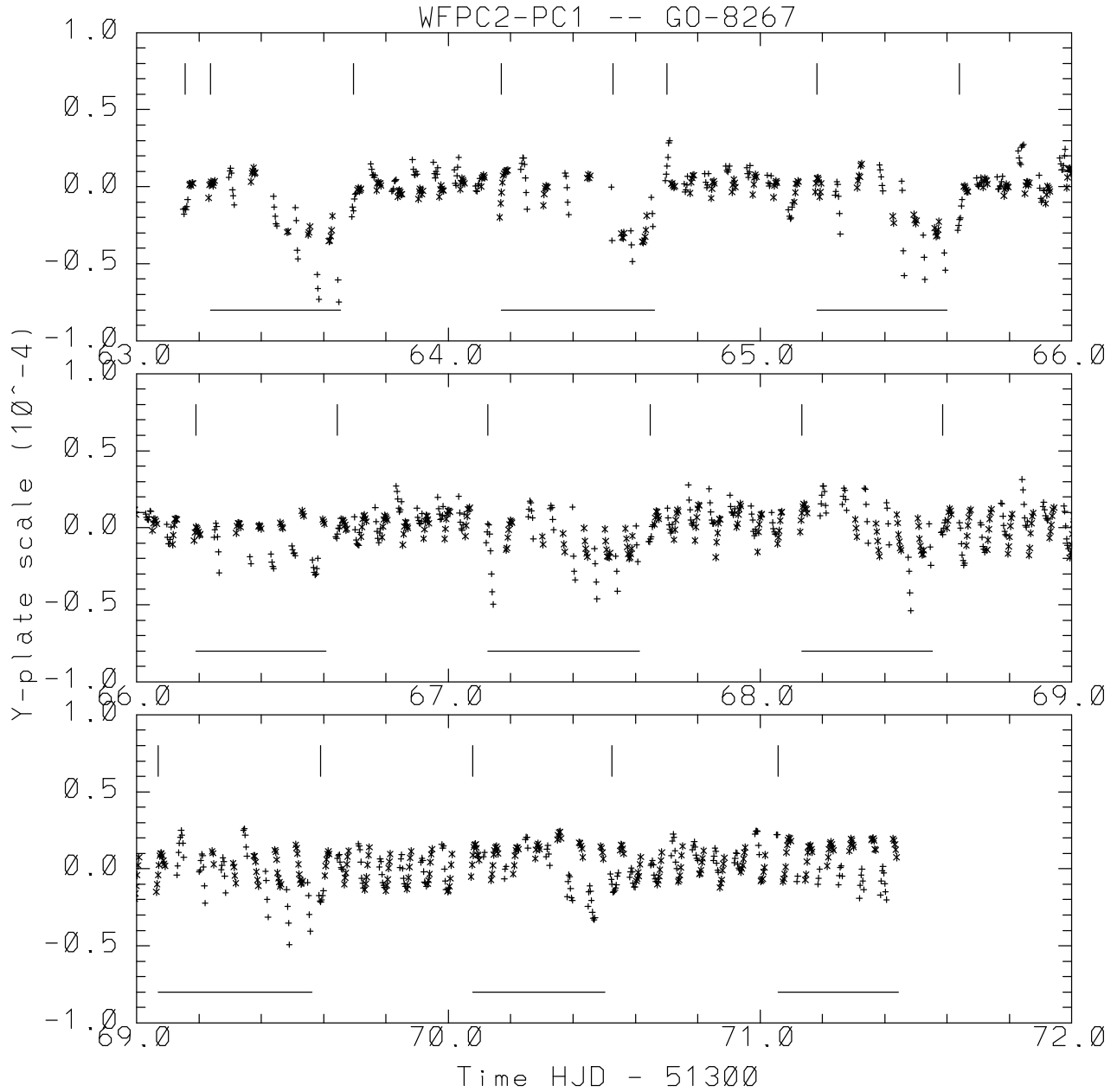


Fig. 6.— Same as Figure 2, but shows the variation of plate scale in the detector y-direction. There is an apparent correlation with times interrupted by the SAA – this may not be real since SAA-orbits *for this program* resulted in use of extended phases of visibility periods relative to standard orbits.

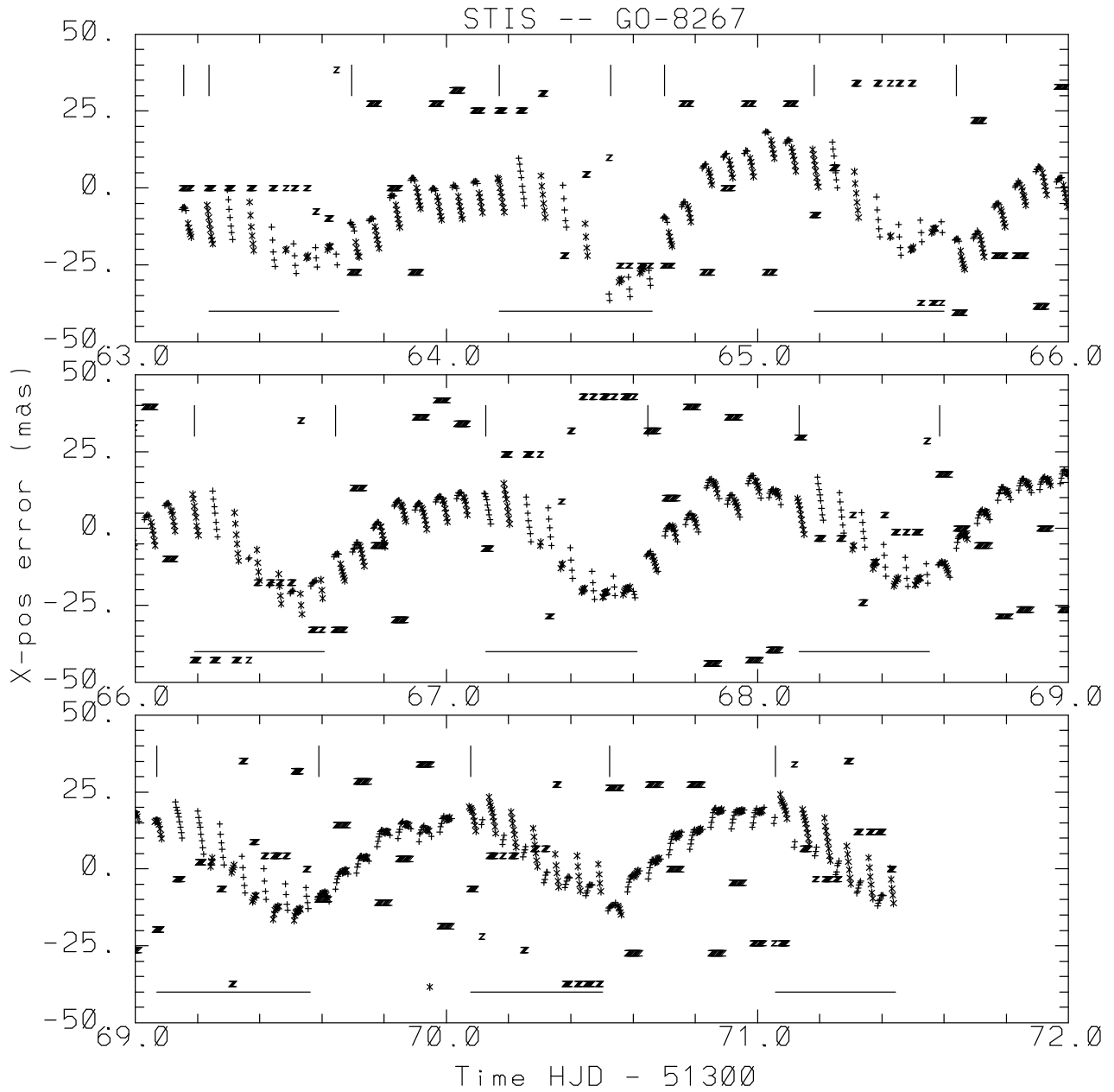


Fig. 7.— This and the next four figures are for the STIS observations taken in parallel with WFPC2 in GO-8267, and these five figures directly correspond to Figures 2 – 6 . It is clear that STIS experiences much larger position drifts, not however from differential velocity aberration. A one day variation perhaps results from thermal fluctuations within STIS as the MAMA detectors are powered off during SAA affected orbits.

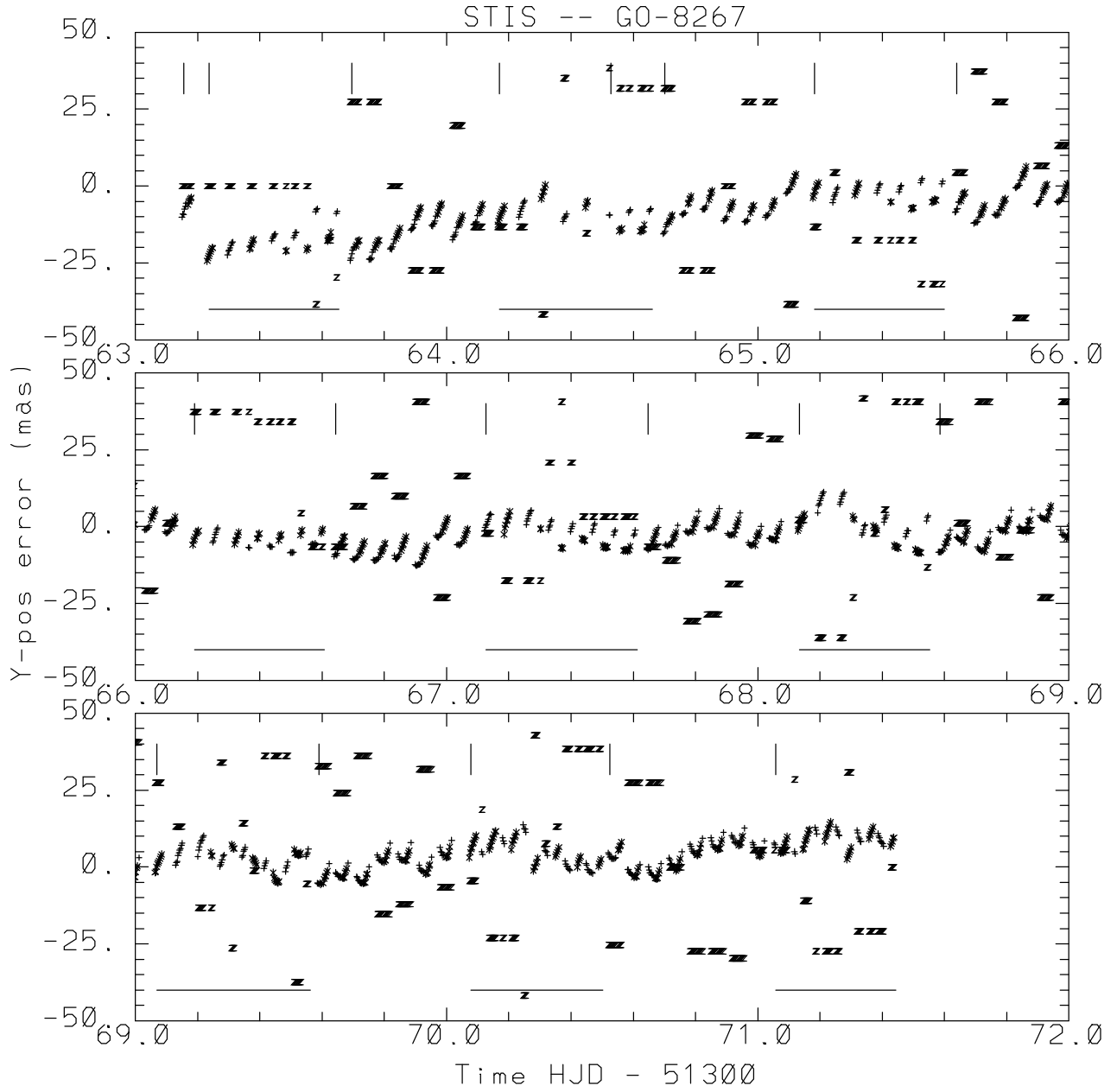


Fig. 8.— Y-position pointing errors for the STIS observations of GO-8267.

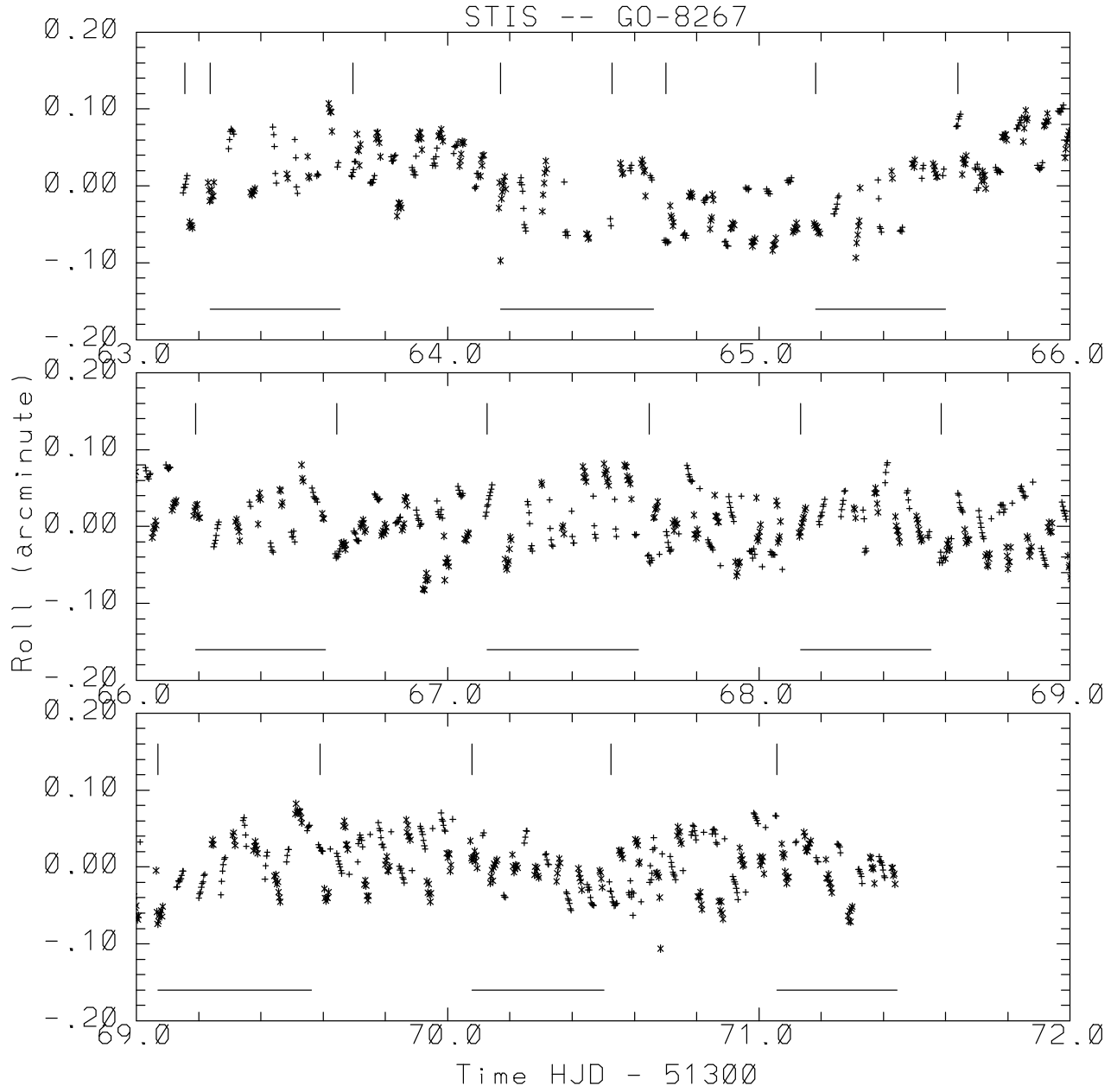


Fig. 9.— The relative roll variations for STIS observations of GO-8267.

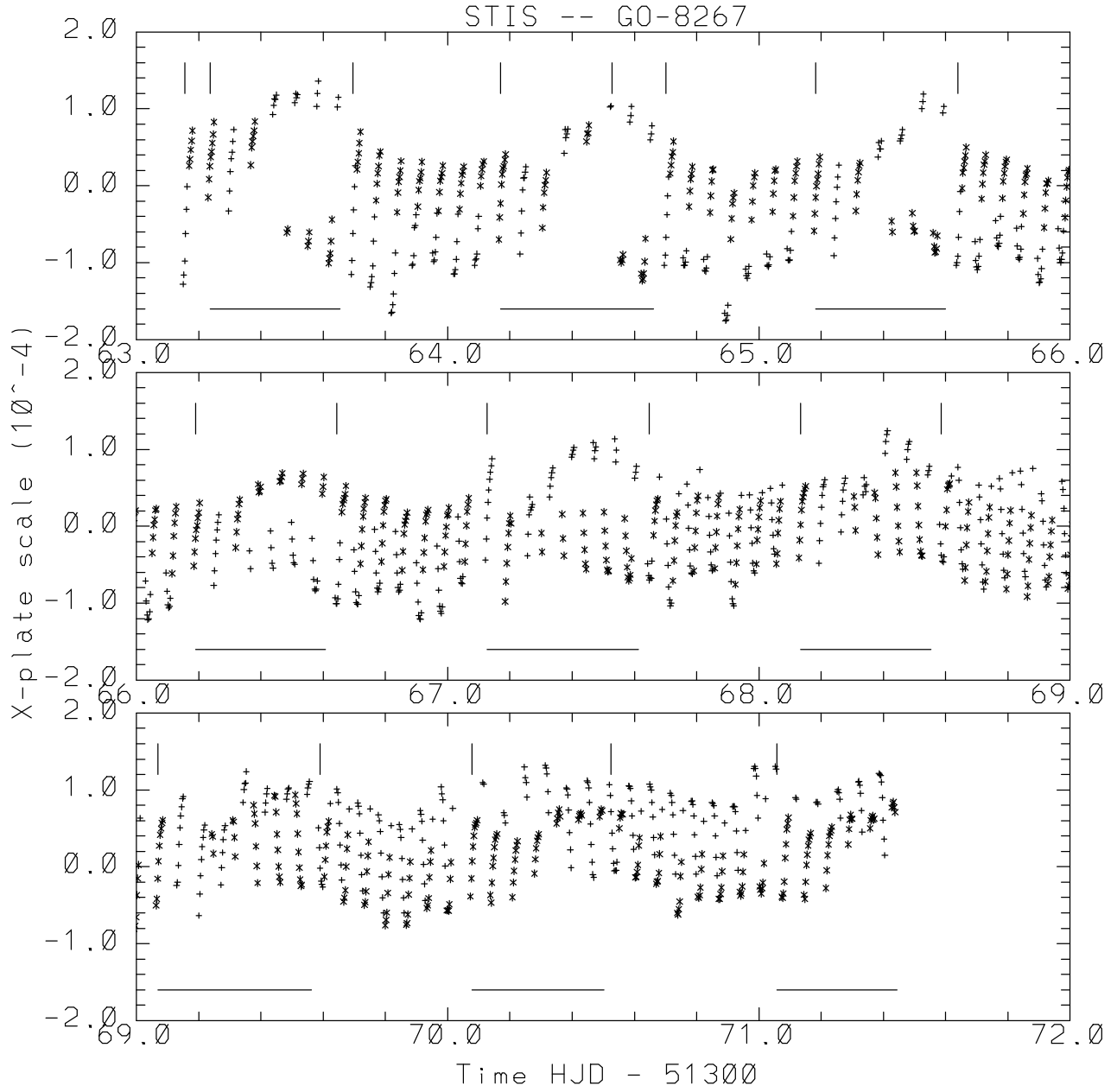


Fig. 10.— Variations of plate scale along detector x-direction for STIS. Note that these are a factor of more than two larger than the PC1 changes with WFPC2 shown in Figure 5, and are much larger than could be explained by differential velocity aberration.

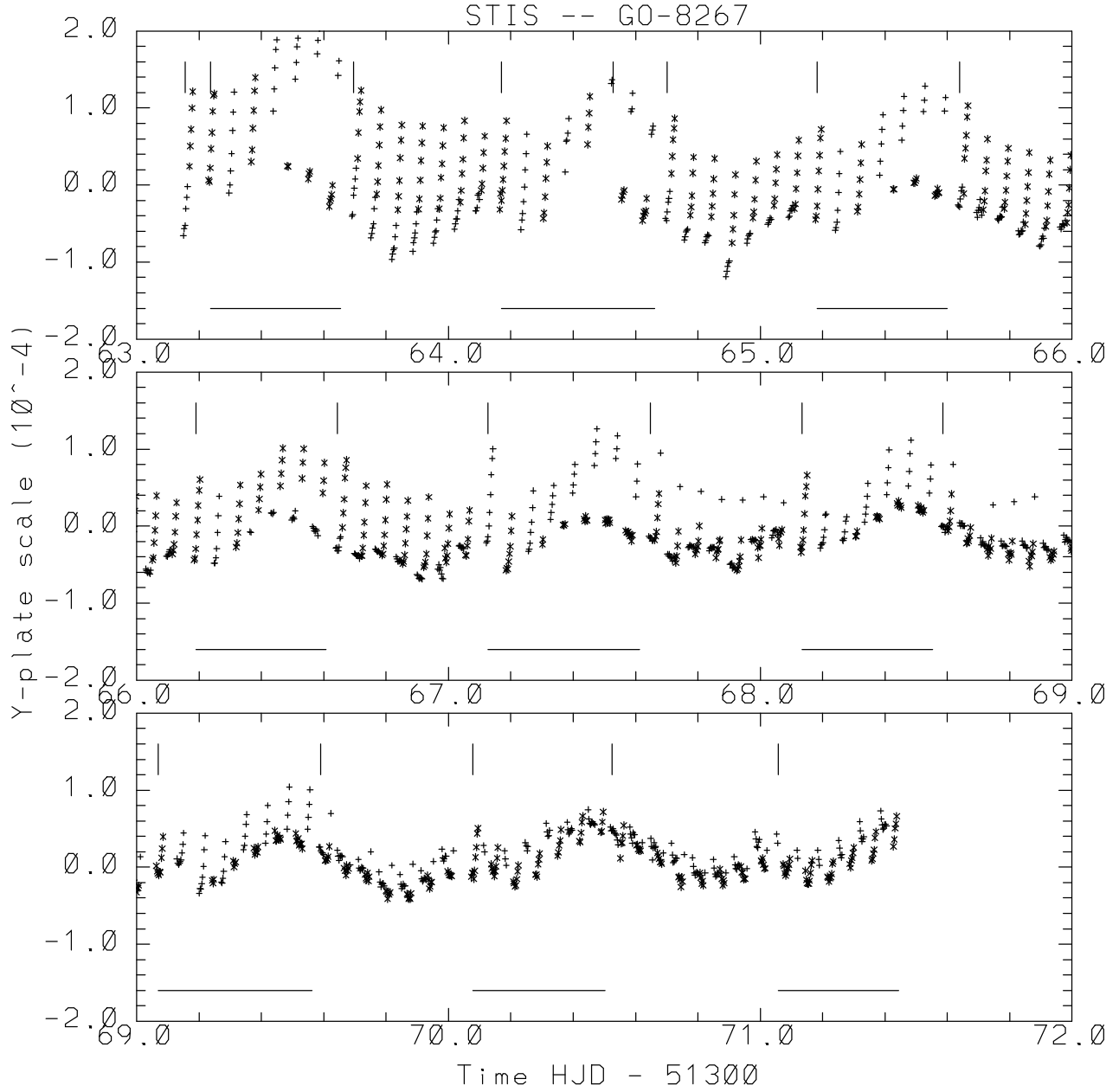


Fig. 11.— Variations of plate scale along detector y-axis for STIS in GO-8267. Note the unique monotonic decrease of *HST*-orbital modulation compared to either WFPC2, or the x-axis on STIS.

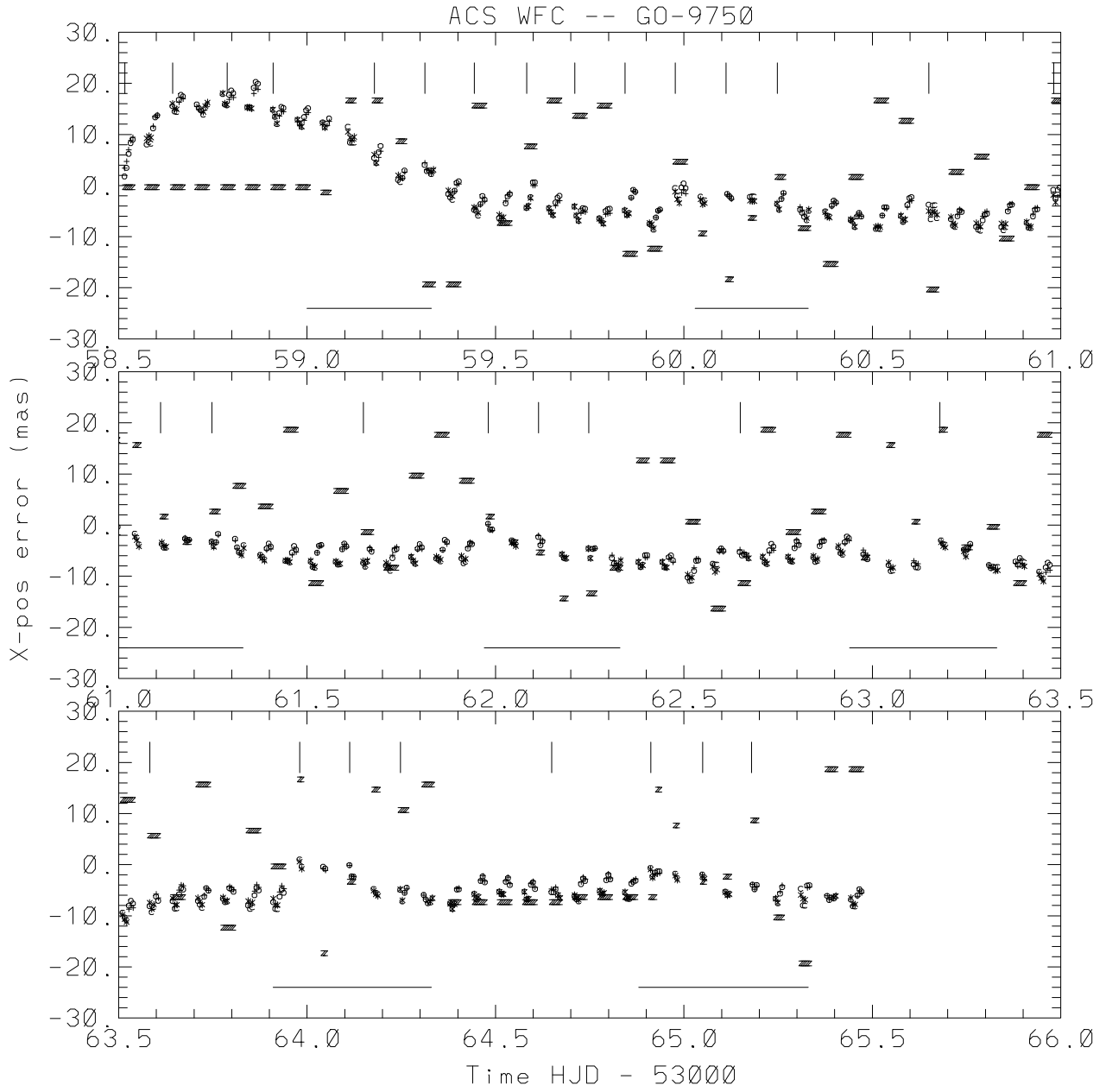


Fig. 12.— This and next four figures show the x, y position errors, roll, and x,y plate scale changes during the 7 days of observations with ACS/WFC for GO-9750 in February 2004. Symbols for the two CCDs are shown separately WFC1 F606W '+' and F814W '\*', with WFC2 F606W 'o' and F814W 'c'. In general the two chips provide very similar results as expected.

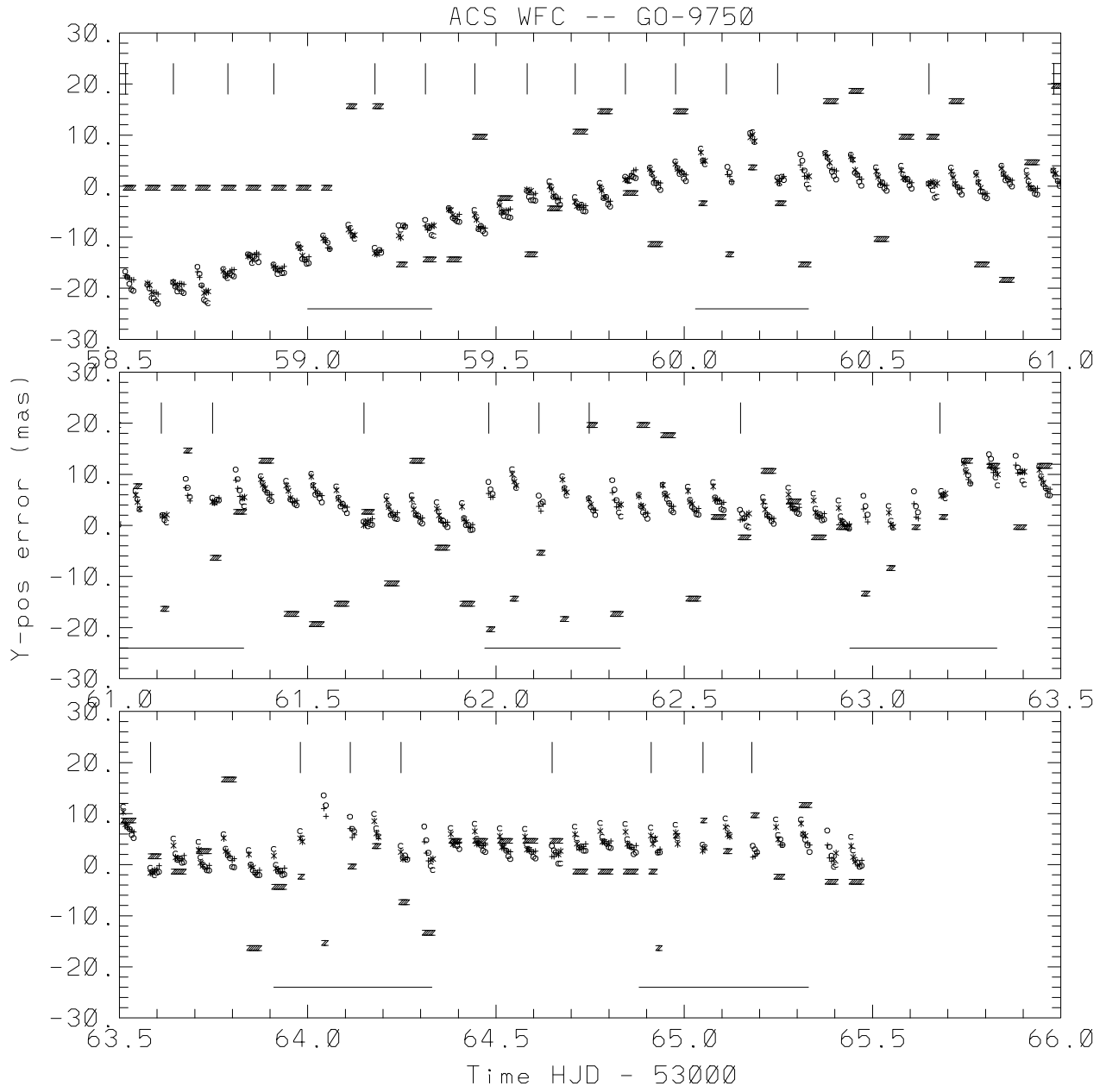


Fig. 13.— Y-position variations for GO-9750 with ACS/WFC.

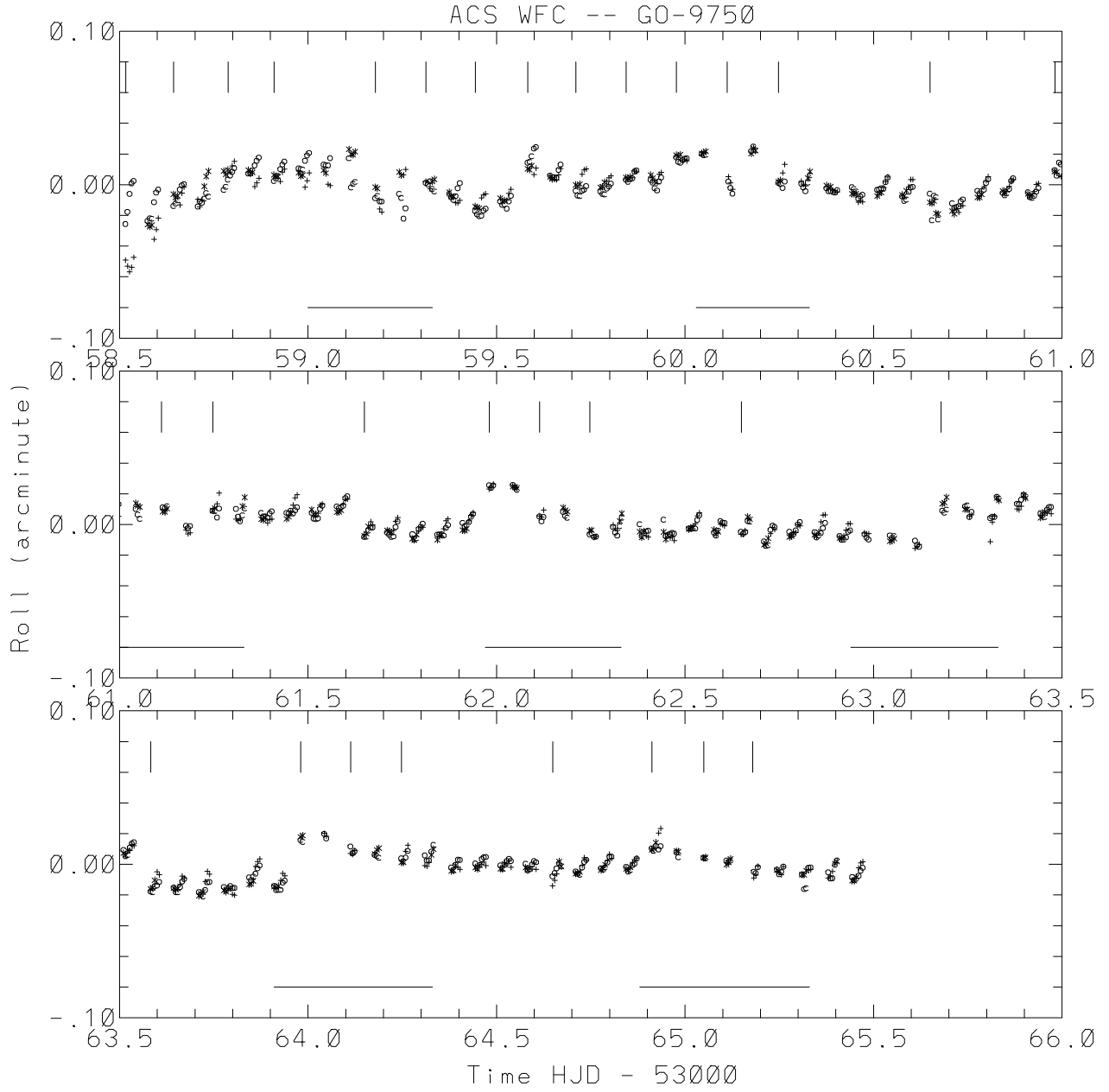


Fig. 14.— Apparent roll variations for the GO-9750 ACS/WFC data.

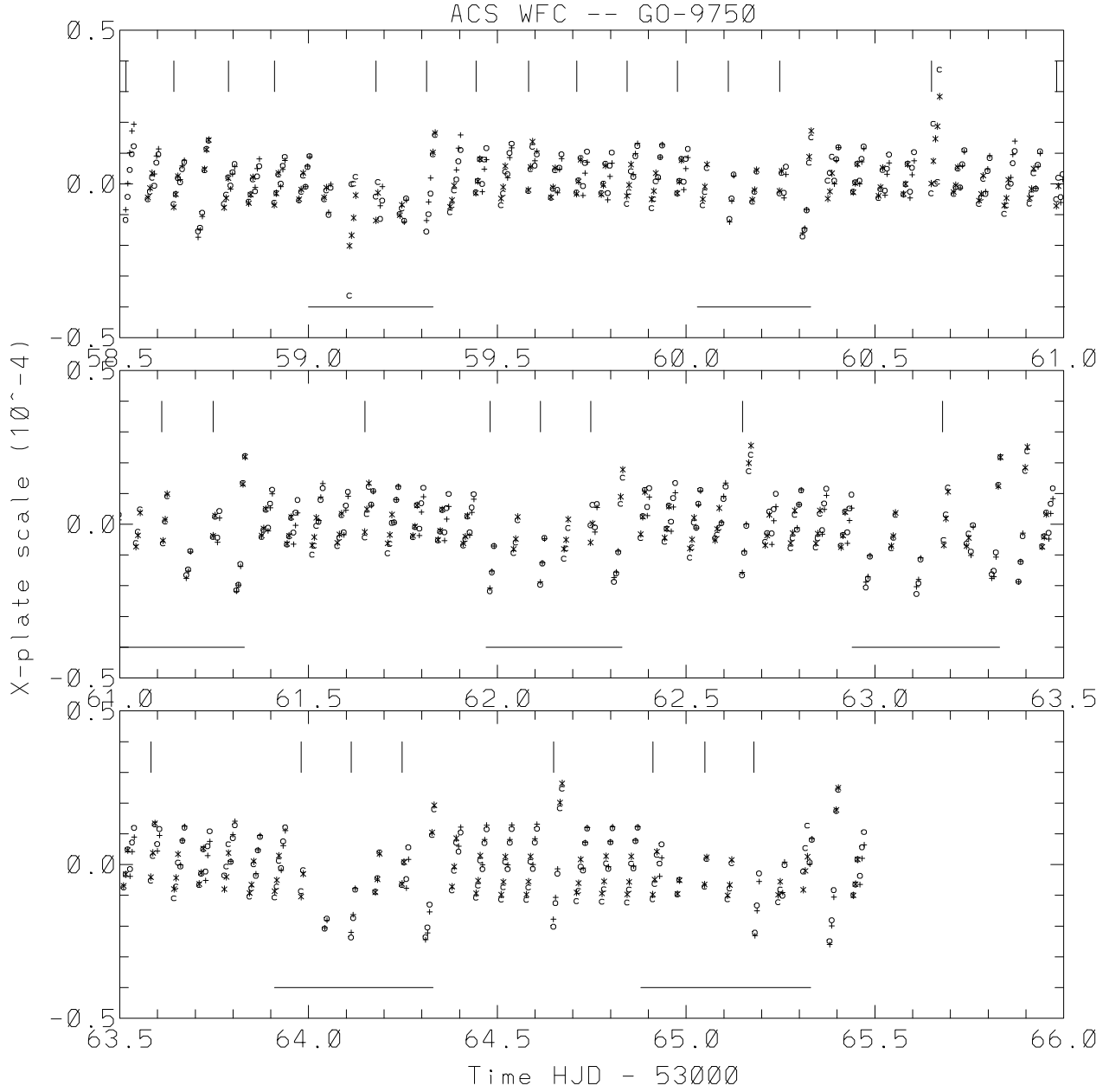


Fig. 15.— Variations of plate scale in x-direction for GO-9750 with ACS/WFC. Unlike WFPC2 and STIS experience, the ACS plate scale variations are at a magnitude consistent with differential velocity aberration.

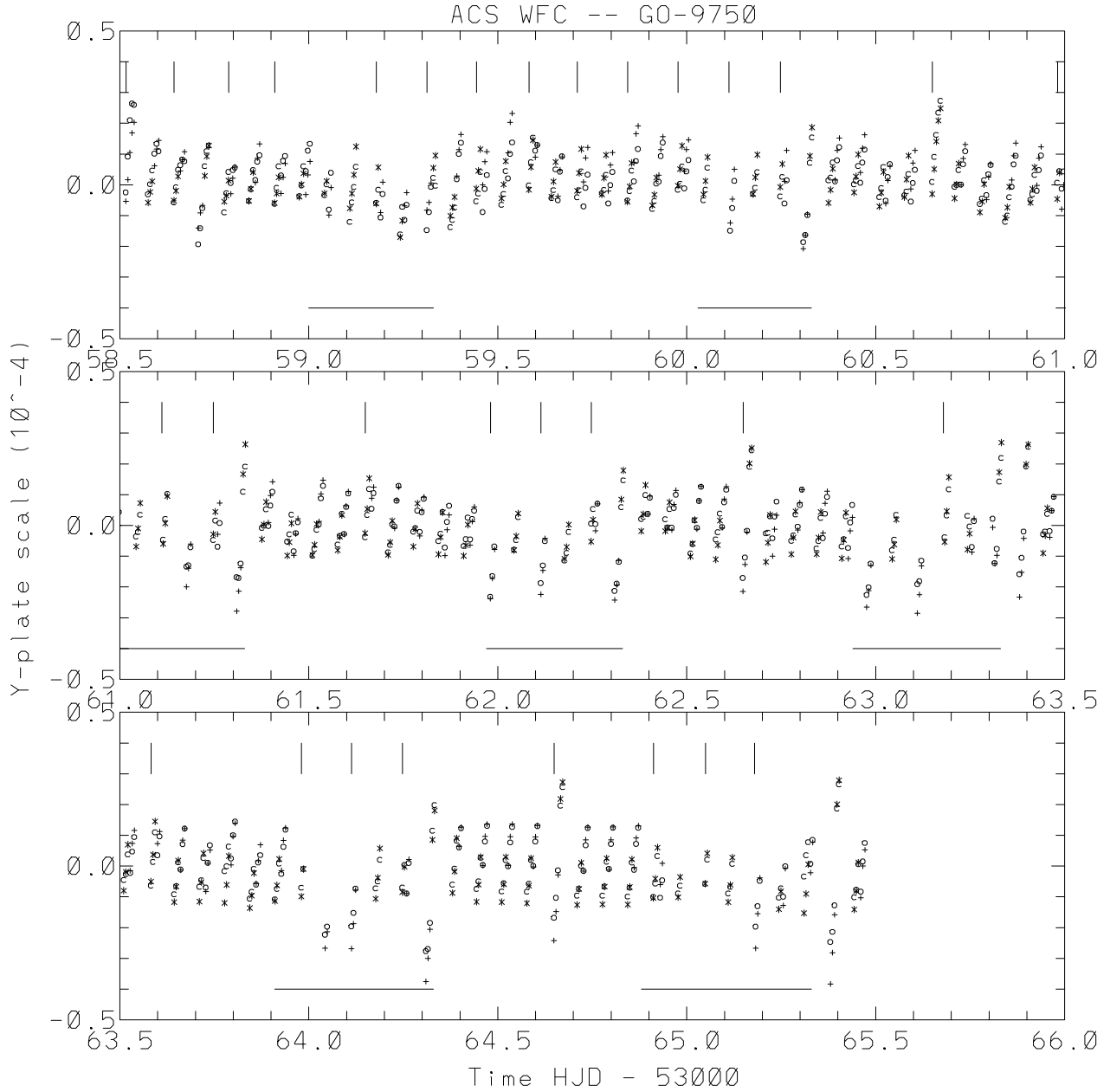


Fig. 16.— Variations of plate scale in the y-direction for GO-9750 with ACS/WFC. As would be expected if variations are due to differential velocity aberration, these variations in y are very similar to those in x shown in the previous figure (since the effect is a simple radial stretch for these small fields of view).

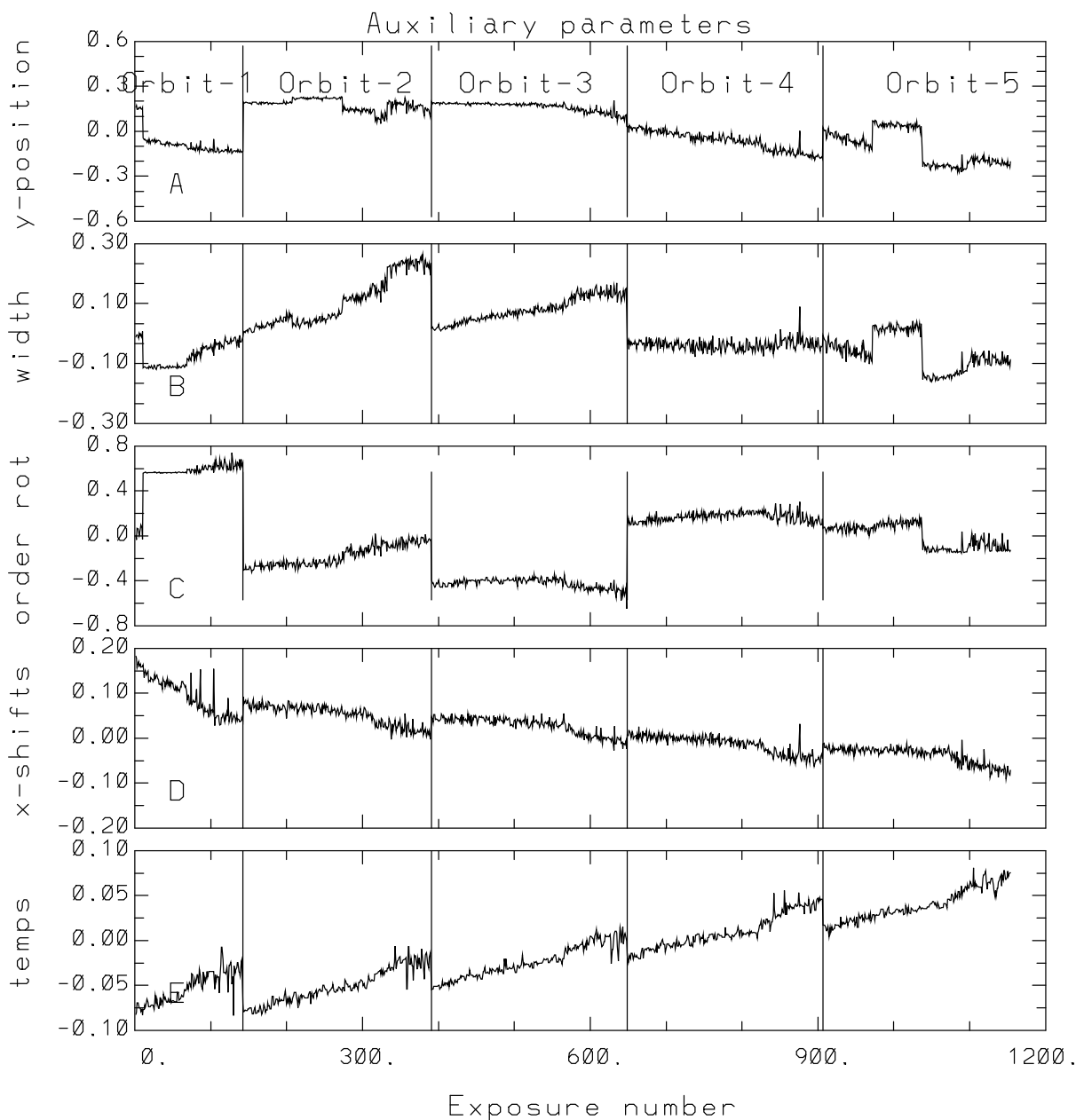


Fig. 17.— Variations of (from top) y-position, order width, rotation of order, x-position and an inferred temperature for NICMOS3 observations with G141 for five consecutive orbits in GO-9832. Units of position and width are in NIC3 pixels of 200 mas. The only observations with changed POS TARGs were the middle quarters of orbits 2 and 5 which were offset by  $\pm 10$  mas relative to all other pointings. Since the NICMOS grating wheel is rotated between orbits, some offsets and rotation of the spectral order may follow from this.